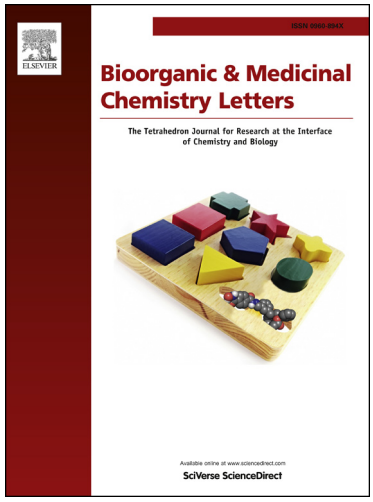

Discovery of 7-azaindole based anaplastic lymphoma kinase (ALK) inhibitors: Wild type and mutant (L1196M) active compounds with unique binding mode

Venkateshwar Rao Gummadi, Sujatha Rajagopalan, Looi Chung Yeng, Mohammadjavad Paydar, Girish Aggunda Renukappa, Bharathi Raja Ainan, Narasimha Rao Krishnamurthy, Sunil Kumar Panigrahi, Kumari Mahasweta, Sangeetha Raghuramachandran, Manoj Rajappa, Anuradha Ramanathan, Anirudha Lakshminarasimhan, Murali Ramachandra, Wong Pooi Fong, Mohammad Rais Mustafa, Srinivas Nanduri, Subramanya Hosahalli

PII: S0960-894X(13)00804-4
DOI: http://dx.doi.org/10.1016/j.bmcl.2013.06.071
Reference: BMCL 20635

To appear in: *Bioorganic & Medicinal Chemistry Letters*

Received Date: 21 March 2013
Revised Date: 3 June 2013
Accepted Date: 25 June 2013

Please cite this article as: Gummadi, V.R., Rajagopalan, S., Yeng, L.C., Paydar, M., Renukappa, G.A., Ainan, B.R., Krishnamurthy, N.R., Panigrahi, S.K., Mahasweta, K., Raghuramachandran, S., Rajappa, M., Ramanathan, A., Lakshminarasimhan, A., Ramachandra, M., Fong, W.P., Mustafa, M.R., Nanduri, S., Hosahalli, S., Discovery of 7-azaindole based anaplastic lymphoma kinase (ALK) inhibitors: Wild type and mutant (L1196M) active compounds with unique binding mode, *Bioorganic & Medicinal Chemistry Letters* (2013), doi: http://dx.doi.org/10.1016/j.bmcl.2013.06.071

Graphical Abstract

Discovery of 7-azaindole based anaplastic lymphoma kinase (ALK) inhibitors: Wild type and mutant (L1196M) active compounds with unique binding mode

Venkateshwar Rao Gummadi[a, §], Sujatha Rajagopalan[a, §], Looi Chung Yeng[b], Mohammadjavad Paydar[b], Girish Aggunda Renukappa[a], Bharathi Raja Ainan[a], Narasimha Rao Krishnamurthy[a], Sunil Kumar Panigrahi[a] , Kumari Mahasweta[a], Sangeetha Raghuramachandran[a], Manoj Rajappa[a], Anuradha Ramanathan[a], Anirudha Lakshminarasimhan[a], Murali Ramachandra[a], Wong Pooi Fong[b], Mohammad Rais Mustafa[b], Srinivas Nanduri[a], Subramanya Hosahalli[a, *]

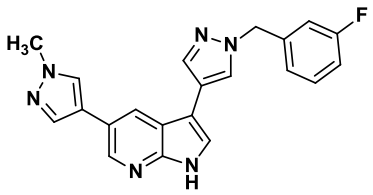

7b IC_{50} = 5.6 nM

A novel series of 7-Azaindole derivatives have been identified as potent ALK inhibitors. Their synthesis and preliminary SAR are described.

Bioorganic & Medicinal Chemistry Letters
journal homepage: www.elsevier.com

Discovery of 7-azaindole based anaplastic lymphoma kinase (ALK) inhibitors: Wild type and mutant (L1196M) active compounds with unique binding mode

Venkateshwar Rao Gummadi[a, §], Sujatha Rajagopalan[a, §], Looi Chung Yeng[b], Mohammadjavad Paydar[b], Girish Aggunda Renukappa[a], Bharathi Raja Ainan[a], Narasimha Rao Krishnamurthy[a], Sunil Kumar Panigrahi[a], Kumari Mahasweta[a], Sangeetha Raghuramachandran[a], Manoj Rajappa[a], Anuradha Ramanathan[a], Anirudha Lakshminarasimhan[a], Murali Ramachandra[a], Wong Pooi Fong[b], Mohammad Rais Mustafa[b], Srinivas Nanduri[a], Subramanya Hosahalli[a, *]

[a]*Aurigene Discovery Technologies Ltd, #39/40, KIADB Industrial Area, Hosur road, Electronic city Phase-II, Bangalore, India, 560100*
[b]*Department of Pharmacology, Faculty of Medicine, University of Malaya, 50603, Kuala Lumpur, Malaysia*

∗ Corresponding author. Tel.: +91 80 71025316; fax: +91 80 28526285; e-mail: hosahalli_s@aurigene.com
§ These authors have contributed equally to this work

ARTICLE INFO

Article history:
Received
Revised
Accepted
Available online

Keywords:
Anaplastic Lymphoma Kinase (ALK)
7-azaindole
Anaplastic Large Cell Lymphoma (ALCL)
Cancer
Karpass 299

ABSTRACT

We have identified a novel 7-azaindole series of Anaplastic Lymphoma Kinase (ALK) inhibitors. Compounds **7b, 7m-n** demonstrate excellent potencies in biochemical and cellular assays. X-ray crystal structure of one of the compounds (**7k**) revealed a unique binding mode with the benzyl group occupying the back pocket, explaining its potency towards ALK and selectivity over tested kinases particularly Aurora-A. This binding mode is in contrast to that of known ALK inhibitors such as crizotinib and NVP-TAE684 which occupy the ribose binding pocket, close to DFG motif.

Anaplastic Lymphoma Kinase (ALK) is a transmembrane receptor tyrosine kinase that belongs to the insulin receptor superfamily. Physiologically ALK is involved in the early development and function of nervous system. However its expression is restricted to the central nervous system in normal adults[1]. Several fusion/mutant proteins of ALK have been implicated in oncogenesis. Nucleophosmin (NPM)-ALK was the first fusion protein to be identified, with the N-terminus of NPM fused to the intracellular domain of ALK. NPM-ALK is present in 30-50% of advanced stage Anaplastic Large Cell Lymphoma (ALCL) patients. Echinoderm microtubule associated protein like 4 (EML4)-ALK, which is identified in 3-7% of lung tumors, has EML4 fused to the intracellular domain of ALK[2]. ALK fusion protein has also been implicated in 30-60% of inflammatory myofibroblastic tumors (IMT)[3]. These fusion proteins mediate ligand-independant oligomerization leading to autophosphorylation and hence constitutive activation of ALK. In addition, overexpression or activating mutations of the protein have been identified in 5-15% of neuroblastoma[4,5]. Recent reports have also identified ALK amplification in 75% of Inflammatory Breast Cancer (IBC) tumor samples that respond to ALK inhibition in pre-clinical models[6]. Oncogenic ALK mediates its effects through activation of PI3K/Akt, Jak/Stat, Raf/Mek/Erk and the PLCγ pathways[7], resulting in increased cell proliferation and resistance to apoptosis. Knock-out studies and the use of selective ALK inhibitors in pre-clinical models have validated this kinase as a potent oncogenic driver in cancers dependant on ALK. Recently Crizotinib a c-Met/ALK dual inhibitor has been given accelerated approval for the treatment of ALK-dependant cancers, further validating the target and the potential therapeutic application of inhibiting this oncogenic kinase. Hence there is compelling evidence for targeting ALK-dependant hematological and solid tumors. In patients, initial response to Crizotinib has been exceptional. However resistance has been known to develop within a year of starting therapy. Several examples of resistance to tyrosine kinase inhibitors (TKIs) have been reported earlier [8,9]. One of the most common mutations has been with the gatekeeper residue observed in TKs such as EGFR (T790M mutation) and BCR-ABL (T315I mutation). Among the first identified resistant mutations in patients treated with Crizotinib has been the critical gatekeeper mutation, leucine to methionine (L1196M) [10]. Hence our focus has been the development of an ALK inhibitor that is potent against both WT and the clinically relevant L1196M mutant form of this kinase[11].

Figure 1.

Screening of an in-house kinase specific library consisting of 3000 compounds resulted in the identification of 7-azaindole compound **1** (Figure 1) as a potent inhibitor of ALK. Compound **1** showed an enzymatic potency of 90 and 141nM against wild type and L1196M mutant ALK[12]. It also showed a cellular potency of 3000nM in the ALK-driven Karpas299 proliferation assay[13]. In addition to encouraging enzymatic and cellular potency, the low molecular weight (354 Da) of compound **1** offered a potential for optimization. Profiling against an in-house panel of kinases showed that compound **1** inhibited Aurora A potently (84% inhibition at 100nM concentration) along with ALK. We initiated the optimization of compound **1** with the objectives of improving biochemical potency against ALK (WT and L1196M), improving cellular activity and selectivity against other kinases particularly Aurora A. Compound **1** was docked (Figure 2) in the published ALK crystal structure (PDB ID: 2XP2) to design new compounds. The model reveals two anchoring hydrogen bond interactions in the hinge region-pyrrole NH with main chain carbonyl of Glu-1197 (G+1) residue and pyridine nitrogen of azaindole scaffold with NH of Met-1199 residue (G+3). Substitution at C5- N-methyl pyrazole and C3-pyrazole of compound **1** occupies solvent exposed region and ribose pocket similar to that of crizotinib, respectively.

Figure 2.

Since the docking mode[14] of compound **1** indicated that the 5th position substitution on azaindole occupies the solvent exposed region, efforts were focused on expanding upon the SAR at the C3 position. A general synthetic scheme of these compounds is shown in Schemes 1 and 2. Compound **2** (5-bromo-3-iodo-1-tosyl-1H-pyrrolo [2, 3-b] pyridine) was coupled with various benzyl substituted pyrazole boronate esters to generate compound **4**[15]. Further coupling of compound **4** with the N-methyl pyrazole boronate ester resulted in compound **6**, which on basic hydrolysis gave the desired product **7**.

Scheme 1.

Alternatively these compounds can also be prepared as shown in Scheme 2. Compound **8** (5-bromo pyrrolo [2, 3-b] pyridine) was coupled with N-methyl pyrazole boronate ester and the resulting compound **9** was iodinated and protected with tosyl to afford key intermediate **11**. Further coupling of **11** with various benzyl substituted pyrazole boronate esters afforded compound **6**, which on basic hydrolysis gave the desired product **7**.

Scheme 2.

Docking of compound **1** (Figure2) suggested that the benzyl group occupies a hydrophobic pocket. Hence we synthesized a set of compounds with fluoro substitution on benzyl group resulting in compounds **7a-c.** Table 1 shows biochemical potency of compounds **7a-c** against ALK and Aurora A kinases as well as potency in Karpass-299 cells. Among these three compounds, **7b** (3-F) appeared to be most potent in enzymatic and cellular assays. Compound **7b** showed significantly enhanced biochemical and cellular potency compared to compound **1** although there was no change in selectivity against Aurora A.

Table 1.

Since compound **7b** with 3-F substitution showed an improvement in potency, we explored various other substitutions at this position of the benzyl group (Table 2). Although several of these compounds were reasonably tolerated it did not show improvement in either biochemical or cellular or selectivity against Aurora A compared to compound **7b**. Compound **7f** showed a significantly reduced potency indicating that bulkier groups are not tolerated at this position although the docking mode of compound suggested there is sufficient space available for this substitution. The reduced cellular potency observed with compound **7g** is presumably because of lack of permeability due to carboxylic acid.

Table 2.

Based on the docking model (Figure 2), the benzyl ring of compound **1** and the tri-substituted phenyl ring of crizotinib, occupy a similar space in the ribose pocket. Although these two moieties are separated by ~ 2 Å, sufficient space appears to be available for substitution on benzyl ring. Hence we started exploring multiple substitutions on benzyl ring of compound **7b**. We synthesized compounds with disubstitutions on the benzyl group as shown in Table 2. Compound **7m** with 3, 5-difluoro substitution showed biochemical and cellular potencies comparable to **7b**.

Although these compounds showed anti-proliferative activity in the functional assay (XTT), we sought to understand their potency against the target in a cellular system. Hence we measured the inhibition of the target pALK. Since Stat3 is one of the primary mediators of ALK activity, we also measured pStat3 levels in cells following compound treatment. Dose dependent inhibition of pALK was determined by in-cell western assay[16], while pStat3 inhibition (for selected compounds) was determined by Western Blot as shown in Figure 3. The corresponding IC_{50} for pALK and pStat3 inhibition is shown in the accompanying Table 3. Inhibition of pALK and pStat3 correlate well with the anti-proliferative activity in the ALK-dependant Karpas 299 cells. Compound **7b** with good biochemical and cellular potency showed the best inhibition of pALK and pStat3. In contrast compound **7c** which showed weaker inhibition of pALK and pStat3 was also weaker in the biochemical and anti-proliferation assays.

Figure 3.

Table 3.

We co-crystallized one of the compounds (**7k**) with ALK kinase domain[17]. The crystallographically determined binding mode of compound **7k** is shown in Figure 4.

Figure 4.

Compound **7k** occupies the ATP binding pocket of ALK. Hydrogen bonding interactions are seen with pyrrole NH to main chain carbonyl of Glu-1197 (G+1) and pyridine nitrogen with main chain amine of Met-1199 (G+3) residue. N-methyl pyrazole moiety of the compound is directed towards the solvent exposed region. This is in agreement with the earlier modeling study (Figure 2) and is similar to binding modes of reported ALK inhibitors e.g. NVP-TAE684 and Crizotinib. Comparison of the X-ray structures of crizotinib and compound **7k** reveal no conformational changes in secondary structure of the protein. Significant movement is observed in some of the side chains of residues including Glu-1167, Lys-1150, and Phe-1165 to accommodate the benzyl ring. Among these, side chain of Glu–1167 shows a maximum of 3.4Å movement. Surprisingly the 2, 5-difluoro substituted phenyl ring occupies a unique binding pocket not predicted by modeling studies. There is a significant difference in the binding mode of compounds in the back pocket region. NVP-TAE684 and Crizotinib occupy ribose binding pocket (close to DFG loop), while compounds reported in 4DCE, 4FNY, 4FNZ structures extend deep into the back pocket adjacent to gate keeper residue[18]. In contrast, the 2, 5-difluoro substituted phenyl ring of compound **7k** occupies a unique binding pocket adjacent to the catalytic Lys. This unique binding mode of compound **7k** is not observed with any of the compounds reported in published ALK co-crystal structures.

Figure 5.

The benzyl group occupies the back pocket surrounded by hydrophobic residues Ileu-1194 and Leu-1196. In addition polar residues like Lys-1150, Glu-1167 and Arg-1275 are in close proximity to this pocket. In this binding mode the 5-F is positioned in close proximity to side chain of Arg-1275 residue while 2-F is positioned near the gate keeper Leu-1196 residue. This unique conformation and the binding mode is afforded by the relative rigidity of the pyrazole moiety at 3rd position and the potential interactions between the substituted phenyl ring and the back pocket residues. In addition, the presence of catalytic Lys-1150 in the close proximity of the pyrazole moiety can also have a stabilizing hydrogen bond interaction. The 3-F substitution on the benzyl group occupies a small hydrophobic pocket created by Ile-1194 (3.2 Å) and Ile-1171 (3.6 Å) residues at the back pocket and appear to be the optimal substitution as shown with compound **7b**. However bulkier substitution like 3-CF_3 (**7f**) at this position is not tolerated because of steric hindrance. The enhanced biochemical potency of compound **7k** with respect to compound **1** appears to be due to the space filling effect of 2,5-difluoro substituted phenyl group.

Most of the synthesized compounds showed very high inhibition of Aurora A kinase activity. ALK kinase activity appears to be the main driver in ALK dependant tumors. Addition of Aurora A has not been shown to have any synergistic/additive effect in these tumors. In addition inhibition of Aurora kinases have been implicated in cardiotoxicity[19].
In order to understand selectivity of these compounds, **7b** was docked in the X-ray structure of a representative Aurora A kinase domain (PDB ID: 2XNG). Docking mode of compound **7b** indicated an interaction of pyrazole nitrogen with catalytic Lys-162, while the benzylic group is placed in the ribose pocket. A similar proximity of the pyrazole nitrogen to catalytic Lys-1150 is also observed in the docking mode of compound **7b** with ALK. However, orientation of pyrazole moiety appears to be slightly different in ALK as compared to Aurora-A. Consequently, pyrazole nitrogen is placed closer to the catalytic Lys-162 in case of Aurora A (3 Å) compared to ALK (4.4 Å). It was hypothesized that disruption of this interaction may result in significant reduction of Aurora A kinase activity, while its impact on ALK activity could be much lesser. Hence we synthesized few substituted pyrazole analogs as shown in Table 4. Interestingly some of these modifications improved selectivity against Aurora A kinase.

Compared to unsubstituted pyrazole, mono and dimethyl pyrazole appear to give better selectivity against Aurora A (**7n**, **7o** & **7q**). Substitution on the benzyl group also appears to have some influence on selectivity. 3,5-difluoro substitution on the benzyl group along with dimethyl substitution on the pyrazole (**7q**) appear to give best selectivity against Aurora A. Docking mode of compound **7q** with Aurora-A is shown in Figure 6. As hypothesized, dimethyl substitution on pyrazole appears to change the orientation of pyrazole moiety, resulting in loss of interaction with catalytic Lys-162. This is also evident from the biochemical activities of compounds **7q** and **7b**. Dimethyl substitution at pyrazole in compound **7q** results in significant loss in Aurora A potency (64 folds) and marginal loss of ALK WT (4 folds) in comparison with compound **7b**.

Figure 6.

Table 4.

In summary screening of a library of compounds resulted in identification of a novel series of azaindole compounds as potent ALK inhibitors. Co-crystal structure of one of the compounds revealed a unique binding mode for azaindole compounds compared to Crizotinib and NVP-TAE684. A combination of SAR and structure-guided approach was employed to optimize initial hit compounds. These compounds showed excellent potency against ALK WT as well as the clinically relevant L1196M mutant enzyme. Some of the compounds showed good cell based potency in both anti-proliferative and mechanistic assays. Dimethyl substitution on right hand side pyrazole ring led to enhanced selectivity against Aurora A kinase as indicated by the crystal structure and docking studies. Further efforts to optimize cellular and ADME properties of these molecules are in progress.

Acknowledgments

This research was supported by HIR grant (H-20001-E00002) from the University of Malaya. The authors are thankful to analytical, IPM department and Sivapriya Marappan of Aurigene Discovery Technologies Ltd for providing support during the research work.

References and notes:

1. Morris, S. W.; Kirstein, M. N.; Valentine, M. B.; Dittmer, K. G.; Shapiro, D. N.; Saltman, D. L.; Look AT. Science **1994**, 263 (5151), 1281.
2. Young Lim Choi.; Kengo Takeuchi.; Manabu Soda.; Kentaro Inamura.; Yuki Togashi.; Satoko Hatano.; Munehiro Enomoto.; Toru Hamada.; Hidenori Haruta.; Hideki Watanabe.; Kentaro Kurashina.; Hisashi Hatanaka.; Toshihide Ueno.; Shuji Takada.; Yoshihiro Yamashita.; Yukihiko Sugiyama.; Yuichi Ishikawa.; Hiroyuki Mano. Cancer Res. **2008**, 68(13), 4971.
3. Gleason, B. C.; Hornick, J. L. J. Clin. Pathology. **2008**, 61, 428.
4. Helena Car´en.; Frida Abel.; Per Kogner.; Tommy Martinsson. Biochem. J. **2008**, 416, 153.
5. Rani E. George.; Takaomi Sanda.; Megan Hanna.; Stefan Fröhling.; William LutherII.; Jianming Zhang.; Yebin Ahn.; Wenjun Zhou.; Wendy B. London.; Patrick McGrady.; Liquan Xue.; Sergey Zozulya.; Vlad Gregor.; Thomas R. Webb.; Nathanael S. Gray.; D. Gary Gilliland.; Lisa Diller.; Heidi Greulich.; Stephan W. Morris.; Matthew Meyerson.; Look, A. T. Nature **2008**, 455(7215), 975.
6. Rabiya S Tuma. J. Natl. Cancer Inst. **2012**, 104 (2), 87.
7. Shaw, A.; Solomon, B. Clin. Cancer. Res. **2011**, 17(8), 2081
8. Ruriko Tanaka.; Shinya Kimura. Exp. Rev. of Anticancer Therapy. **2008**, 8(9), 1387.
9. Cai-Hong Yun.; Kristen E. Mengwasser.; Angela V. Toms.; Michele S. Woo.; Heidi Greulich.; Kwok-Kin Wong.; Matthew Meyerson.; Michael J. Eck. PNAS. **2008**, 105 (6), 2070.
10. Young Lim Choi.; Manabu Soda.; Yoshihiro Yamashita.; Toshihide Ueno.; Junpei Takashima.;Takahiro Nakajima.; Yasushi Yatabe.; Kengo Takeuchi.; Toru Hamada.; Hidenori Haruta.; Yuichi Ishikawa.; Hideki Kimura.; Tetsuya Mitsudomi.; Yoshiro Tanio.; Hiroyuki Mano. N. Eng. J. Med. **2010**, 363(18), 1734.
11. Refer Supplementary data, section C; part-I
12. In vitro enzyme assays: The ALK WT activity was determined, in a 384-well TR-FRET format using recombinant human ALK enzyme (Cat# 08-518, Carna Biosciences) and Ultra Light Poly GT (Cat# TRF 0100D, Perkin Elmer) as a substrate. The final assay conditions were 50 mM HEPES pH 7.1, 10 mM MgCl2, 2 mM MnCl2, 0.01% BSA, 2.5 mM DTT, 0.1 mM Na3 VO4, 40 nM Ultra Light Poly GT, 2.5 ng ALK WT enzyme, 1µM ATP and 125 nM Lance Eu-W1024 labeled anti phospho tyrosine antibody (Cat# AD0203, Perkin Elmer) in 384 well format. The assay reaction time was 30 minutes after which the antibody detection mix is added. The L1196M mutant ALK assay was done in a similar format. Mutant enzyme was from Carna Biosciences (Cat# 08-529) and 0.5µM ATP was used in the assay buffer. The inhibitory activity against Aurora A was assessed by examining the amount of ATP formed using Kinase Glo system (Cat #

V1931, Promega) in the presence of 2μM ATP and Kemptide as substrate.
13. In vitro cell-based assays: Karpas 299 cells were treated with various concentrations of compound for 72h to determine cell growth. Inhibition of proliferation was determined using XTT.
14. Schrodinger suite of software (Schrodinger suite 2012 release) was used for all modeling study. ALK kinase domain (PDB ID: 2XP2 & 2NXG) were prepared using protein preparation wizard. This process takes care of hydrogen atom addition, correction of missing side chains, finding accurate tautomeric state of residues like Histidine at specified pH (pH adjusted to 7.4) and geometric optimization of hydrogen atoms. Similarly 3-D structure of all synthesized compounds were prepared using ligprep module (Version 2.5) prior to docking. Docking was carried out using Glide. Top ranked pose was shortlisted for analysis. All figures corresponding to docking and x-ray structure were generated using Pymol (version 1.5) visualization software from Schrodinger.
15. Semghee Hong; Jinhee Kim; Ju Hyeon Seo; Kyung Hee Jung; Soon-Sun Hong; Sungwoo Hong. J. Med. Chem. **2012**, 55(11), 5337.
16. Briefly Karpas 299 cells were treated with various concentrations of compound for 1h following which they were fixed, permeabilized and inhibition of pALK was determined by in-cell western. For western blotting: Briefly, 4 × 105 Karpas cells were treated with test compound or positive control Crizotinib at the indicated doses for 6 hours. Next, cells were harvested and lysed in RIPA buffer (Santa Cruz). 30 μg of total cell lysates were loaded onto 10% polyacrylamide gel and transferred to microporous polyvinylidene difluoride (PVDF) membrane (Milipore). Immunoblotting was performed with anti-Stat3 and anti-phospho Stat3 (Tyr705) (Cell Signaling Technology, Danvers, MA) antibodies. Membranes were detected using ECL Plus Chemiluminescence Reagent (Amersham, Chalfont, UK).
17. ALK protein was expressed and purified as reported in Biochem. J. **2010**, 430 (3), 425. Freshly purified protein was incubated over night at 4^{o}C with AUAK-39 (in-house compound, structure not disclosed) at 1: 2 ratio. Protein was concentrated to 7mg/ml and crystallization was set up in and around the reported conditions. Crystals were obtained in most of the drops. Crystals were soaked with compound 7k at 1mM concentration for 3 nights before data collection. The crystals were flash frozen at 100K using 20% glycerol as cryo-protectant. The diffraction data were collected using in-house Rigaku RU300 X-ray generator with R-AXIS IV ++detector to a maximum resolution of 2.5 Å. Indexing, integration and scaling were performed using DENZO and SCALEPACK. The structure was solved by molecular replacement (MR) method using the reported ALK structure (PDB Code; 2XP2). Model building and ligand fitting were done using COOT and refinement was carried out using REFMAC 5.2.0001 software. The final model is complete except for some residues due to poor electron density. These missing residues are Gly1123-All1130 (P-loop region), Ser1136-Leu1145, Pro1153-Ala1164, Ala-1214-Leu1221, Tyr1278-Cys1288 and Ala1300-Gly1304.
18. Refer Supplementary data, section C; part-II
19. Thomas Force.; Kyle L. Kolaja. Nat. Rev. Drug Disc. **2011**, 10, 111.

Supplementary data

Supporting information is attached as a separate file.

Table 1. SAR of halo substituted benzyl group

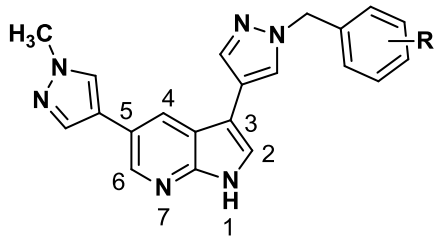

Compound	R	ALK WT IC_{50} [a] nM	ALK (L1196M) IC_{50} [a] nM	Aurora A % inhibition at 100nM	Karpass-299 cell IC_{50} [b] nM
1	H	90	141	84	3000
7a	2-F	85	223	64	2088
7b	3-F	5.6	35	84	466
7c	4-F	70	256.4	74	1781

[a] IC_{50} values determined by TR-FRET; see ref-12
[b] IC_{50} values determined by XTT; see ref-13

Table 2. SAR of the substituted benzyl group

Compound	R	ALK WT IC_{50} [a] nM	ALK (L1196M) IC_{50} [a] nM	Aurora A % inhibition at 100nM	Karpass-299 cell IC_{50} [b] nM
1	H	90	141	84	3000
7b	3-F	5.6	35	84	466
7d	3-Cl	30	143	87	855
7e	3-CN	32	150	85	1609
7f	3-CF_3	247	465.4	84	1008
7g	3-COOH	98	811	ND	>10000
7h	3-NO_2	70	ND	ND	1852
7i	3-NH_2	28	ND	ND	3627
7j	3-OH	41	200.5	93	3363
7k	2,5-difluoro	29	124	75	1200
7l	3,4- difluoro	84	379	84	2261
7m	3,5- difluoro	6	47	74	663.8

[a] IC_{50} values determined by TR-FRET; see ref-12
[b] IC_{50} values determined by XTT; see ref-13, ND – Not determined

Table 3. Comparison of potency of the compounds in functional (XTT) and mechanistic (pStat3 inhibition) assays in Karpas 299 cells. IC_{50} for pStat3 was determined by densitometric evaluation of western blots

Compound	ALK WT IC_{50} nM	pALK IC_{50} (nM)	pStat3 IC_{50} (nM)	XTT IC_{50} (nM)
7b	5.6	219.5	138.5	466
7c	70	3914	3011	1781
7d	30	3121	985.6	855
7k	29	900	1592	1200
7l	84	3300	985.6	2261

Table 4. SAR towards Aurora A selectivity

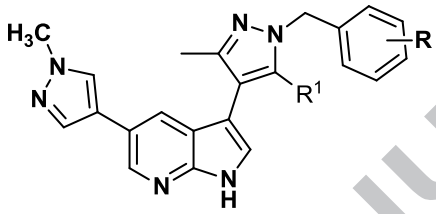

Compound	R	R^1	ALK WT IC_{50} [a] nM	ALK (L1196M) IC_{50} [a] nM	AuroraA IC_{50} nM	Fold selectivity
7b	Shown in Table 1		5.6	35	11.8	2
7n	3-F	H	6	56	37.13	6
7o	3-F	CH_3	31	274.9	355.9	11
7p	2,5-difluoro	CH_3	63	428	216.2	3
7q	3,5- difluoro	CH_3	26	310.2	768.3	30

[a] IC_{50} values determined by TR-FRET; see ref-12

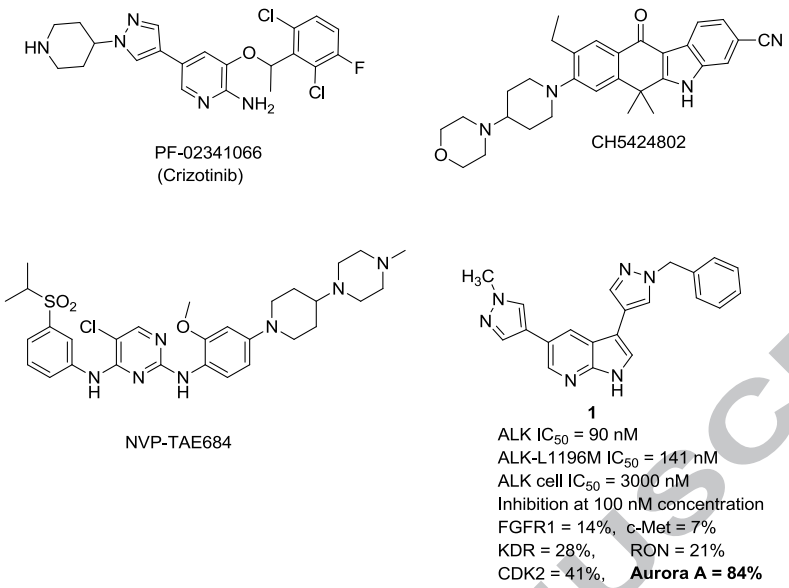

Figure 1. Some of the reported ALK Inhibitors and 7-Azaindole derivative

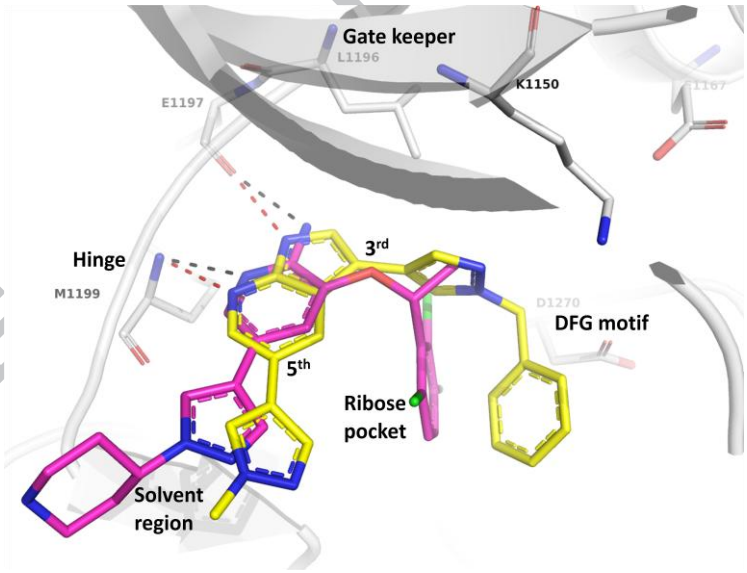

Figure 2. Docking model of compound **1** (yellow) in the X-ray structure of crizotinib bound ALK (PDB ID: 2XP2). Critical hinge hydrogen bond interactions are shown in dotted lines for compound **1** and Crizotinib (magenta). Picture made with Pymol (version 1.5) visualization software.

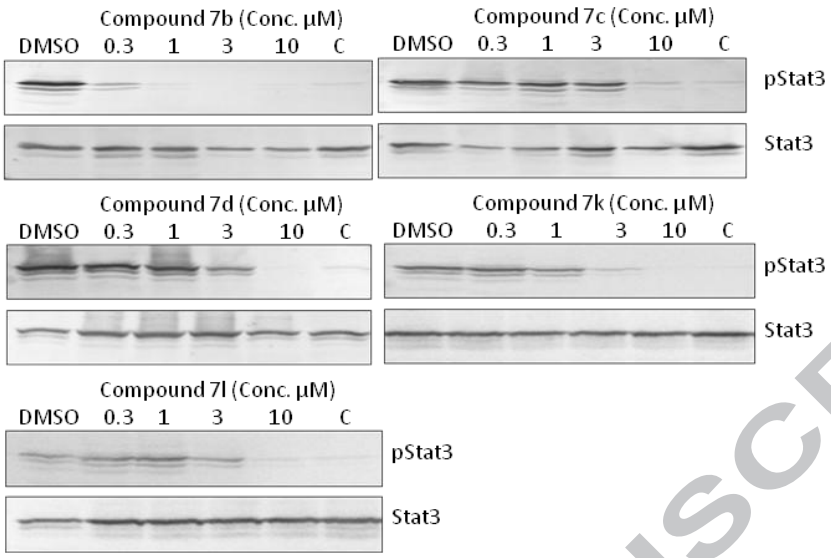

Figure 3. Suppression of Stat3 phosphorylation by ALK inhibitors in Karpas 299. The cells were treated with compounds **7b**, **7c**, **7d**, **7k**, **7l** at the indicated concentrations or known inhibitor Crizotinib at 10 μM (C) for 6 hours. Cell lysates were harvested and evaluated for levels of total and phospho-Stat3 by Western blotting.

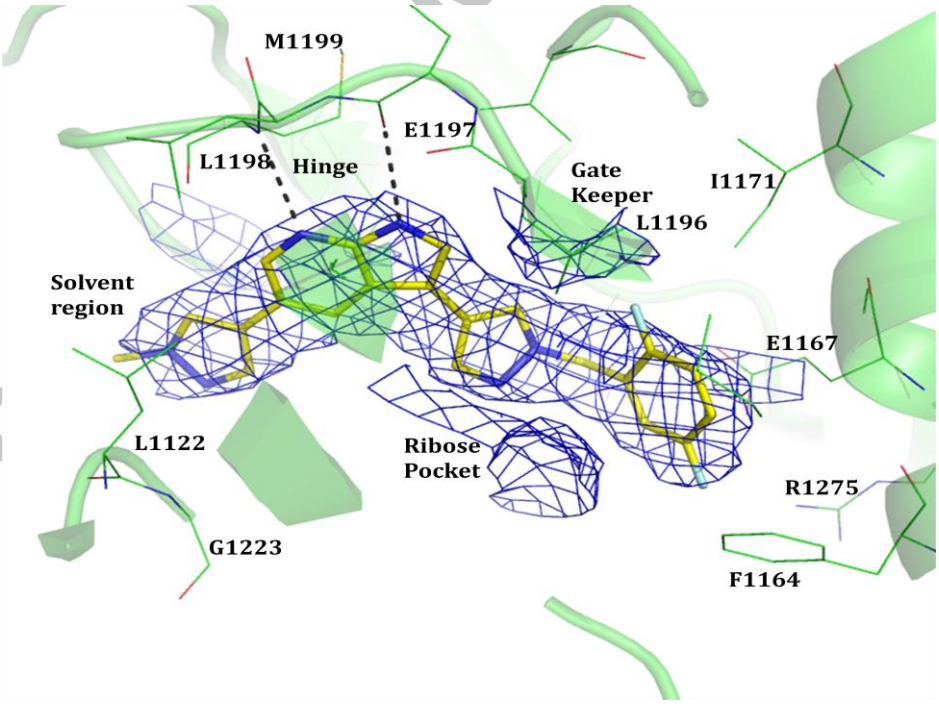

Figure 4. Co-crystal structure of compound **7k** (yellow) in complex with ALK kinase domain (PDB ID: 4J0A). Hydrogen bond interactions are represented by dotted lines and the active site residues are labeled. The 2Fo-Fc electron density map contoured at 1σ level for the bound 7k compound is shown as mesh (blue).

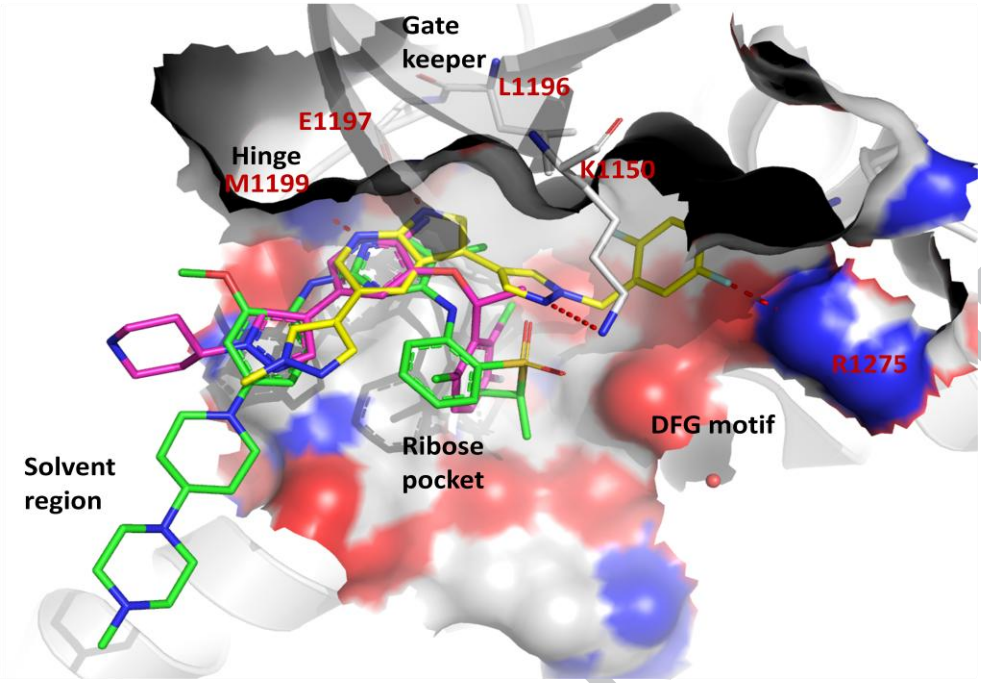

Figure 5. Overlay of X-ray structures of ALK showing critical differences in the binding modes of compounds. Compound **7k** (yellow), Crizotinib (magenta) and NVP-TAE684 (green).

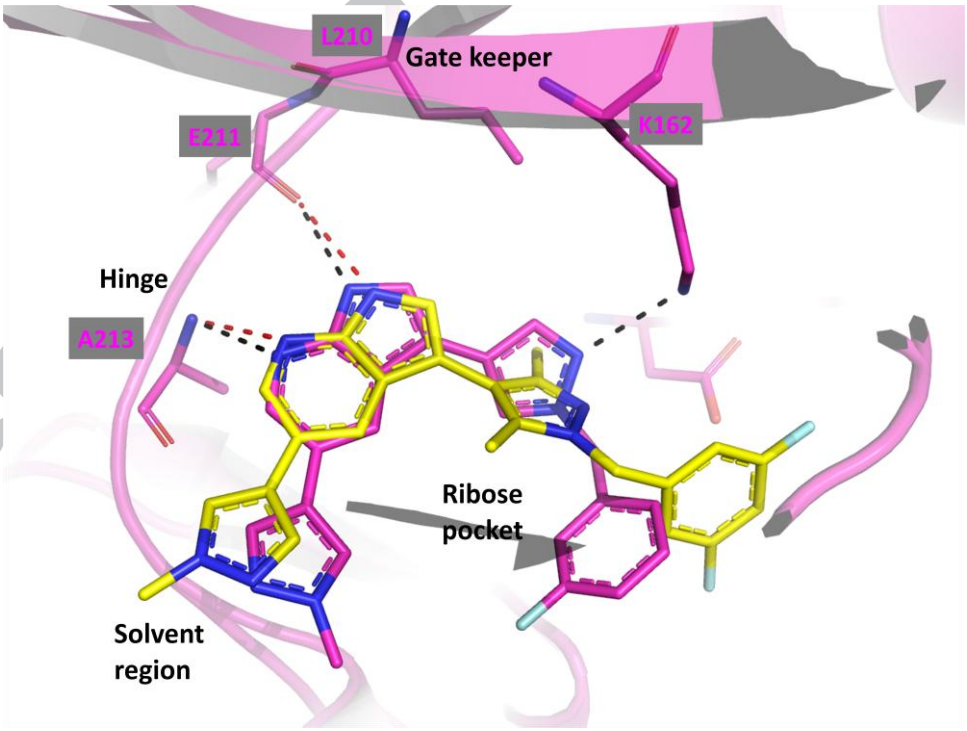

Figure 6. Docking model of **7b** (magenta) and **7q** (yellow) shown in Aurora A kinase domain. Critical differences in binding model of compound **7b** and **7q** are highlighted.

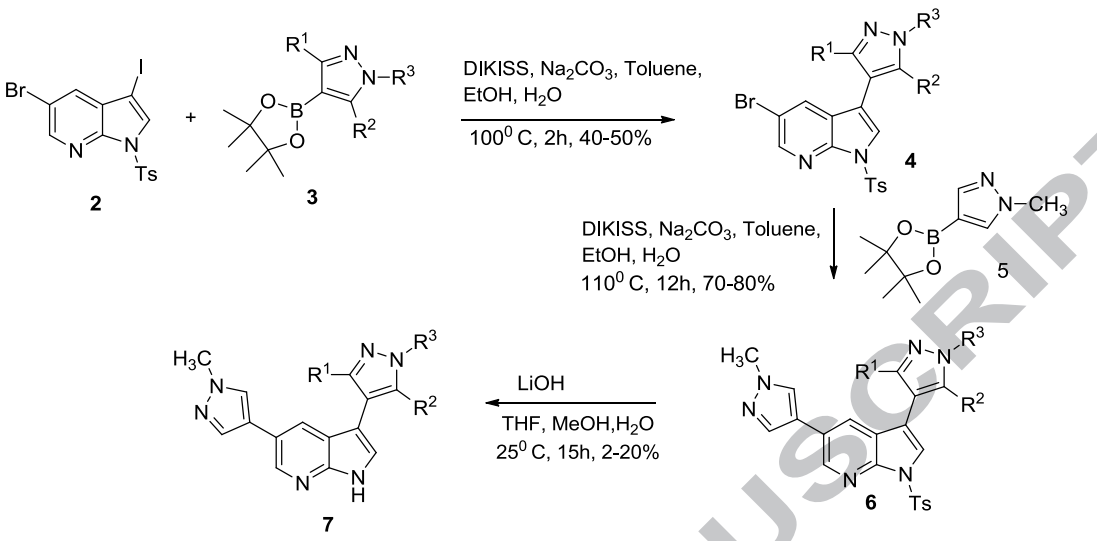

Scheme 1. General synthesis of 3, 5-disubstituted 7-azaindoles

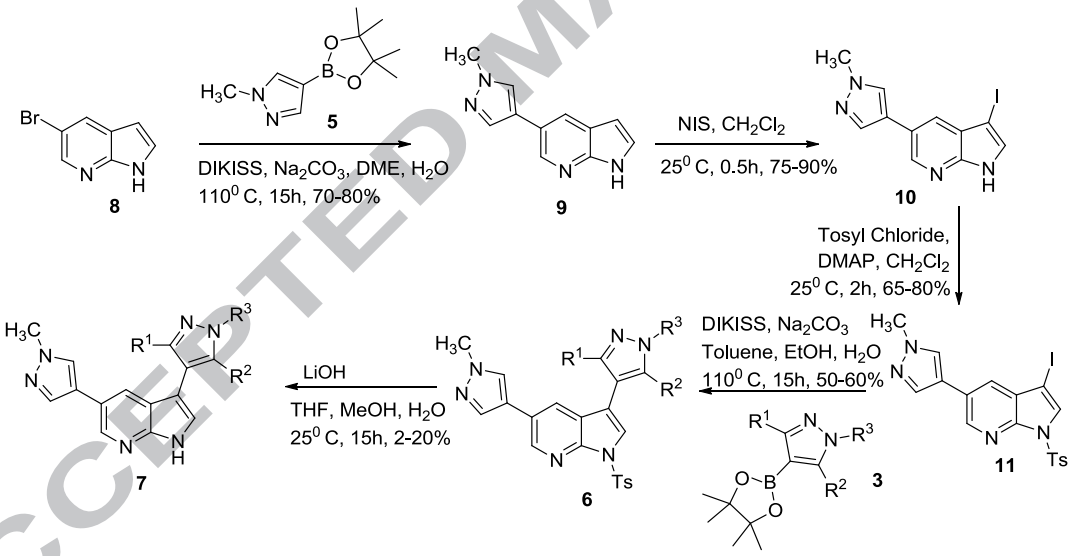

Scheme 2. General synthesis of 3, 5-disubstituted 7-azaindoles